





High-Throughput Screening Platform To Identify Inhibitors of Protein Synthesis with Potential for the Treatment of Malaria

Fabio Tamaki,^a Fabio Fisher,^b Rachel Milne,^a Fernando Sánchez-Román Terán,^b Natalie Wiedemar,^a Karolina Wrobel,^a Darren Edwards,^a Hella Baumann,^b  Ian H. Gilbert,^a Beatriz Baragana,^a Jake Baum,^{b,c}  Susan Wyllie^a

^aWellcome Centre for Anti-Infectives Research, School of Life Sciences, University of Dundee, Dundee, United Kingdom

^bDepartment of Life Sciences, Imperial College London, London, United Kingdom

^cSchool of Medical Sciences, University of New South Wales, New South Wales, Sydney, Australia

Fabio Tamaki and Fabio Fisher contributed equally to this article. Author order was determined by the corresponding authors after negotiation.

ABSTRACT Artemisinin-based combination therapies have been crucial in driving down the global burden of malaria, the world's largest parasitic killer. However, their efficacy is now threatened by the emergence of resistance in Southeast Asia and sub-Saharan Africa. Thus, there is a pressing need to develop new antimalarials with diverse mechanisms of action. One area of *Plasmodium* metabolism that has recently proven rich in exploitable antimalarial targets is protein synthesis, with a compound targeting elongation factor 2 now in clinical development and inhibitors of several aminoacyl-tRNA synthetases in lead optimization. Given the promise of these components of translation as viable drug targets, we rationalized that an assay containing all functional components of translation would be a valuable tool for antimalarial screening and drug discovery. Here, we report the development and validation of an assay platform that enables specific inhibitors of *Plasmodium falciparum* translation (P_FVT) to be identified. The primary assay in this platform monitors the translation of a luciferase reporter in a *P. falciparum* lysate-based expression system. Hits identified in this primary assay are assessed in a counter-screen assay that enables false positives that directly interfere with the luciferase to be triaged. The remaining hit compounds are then assessed in an equivalent human IVT assay. This platform of assays was used to screen MMV's Pandemic and Pathogen Box libraries, identifying several selective inhibitors of protein synthesis. We believe this new high-throughput screening platform has the potential to greatly expedite the discovery of antimalarials that act via this highly desirable mechanism of action.

KEYWORDS *Plasmodium*, malaria, *in vitro* translation, protein synthesis, drug discovery, antimalarials

Malaria is a life-threatening disease that results in more than 400,000 deaths every year, many of which occur among children under the age of 5 years (1). The disease results from infection with unicellular, protozoan parasites from the genus *Plasmodium*, with the vast majority of deaths caused by *Plasmodium falciparum* and *P. vivax*. Current front-line therapies for malaria are under constant threat from the emergence of drug resistance (2, 3). The current standard of care for the treatment of malaria, recommended by the World Health Organization (WHO), is reliant upon artemisinin-based combination therapies (ACTs) (4). However, clinical artemisinin resistance is now prevalent across Southeast Asia (5) and sub-Saharan Africa (6), threatening these combination therapies. Thus, there is a pressing need for new and effective drugs to provide chemoprotection, prevent transmission, and treat (*vivax*) relapse.

The development of new drugs capable of treating this devastating parasitic disease has been confounded by a number of factors. The life cycle of the *Plasmodium* parasite is

Copyright © 2022 Tamaki et al. This is an open-access article distributed under the terms of the [Creative Commons Attribution 4.0 International license](https://creativecommons.org/licenses/by/4.0/).

Address correspondence to Jake Baum, jake.baum@unsw.edu.au, or Susan Wyllie, s.wyllie@dundee.ac.uk.

The authors declare no conflict of interest.

Received 11 February 2022

Returned for modification 4 April 2022

Accepted 3 May 2022

Published 1 June 2022

extremely complex. Following initial transmission via the bite of the *Anopheles* mosquito, sporozoites infect the hepatocytes of the host liver. Parasites replicate and differentiate within hepatocytes prior to entering the bloodstream, where merozoites infect red blood cells. Intraerythrocytic infection is characterized by a rapid expansion of the parasite population (schizogony). At this stage, some parasites differentiate into sexual forms (gametocytes) that can be taken up through the bite of a mosquito and transmitted to other humans. Long-term control of malaria will likely require the development of multiple compounds that demonstrate activity against multiple parasite life cycle stages, extremely challenging in terms of drug discovery. In addition, antimalarial drug discovery has been hindered by the general lack of robustly validated drug targets in *Plasmodium*, severely limiting target-focused screening programs.

One area of *Plasmodium* metabolism that has proven relatively rich in exploitable antimalarial targets is protein synthesis. Doxycycline is widely used for malaria chemoprophylaxis and assumed to act through inhibition of parasite protein synthesis via binding to the 30S ribosomal subunit. The fungal secondary metabolite cladosporin, a potent inhibitor of *Plasmodium* growth in blood and liver stages, specifically targets lysyl-tRNA synthetase (LysRS) (7). Optimization of a chromone hit identified in a biochemical screen led to the first *P. falciparum* LysRS (PfLysRS) inhibitor with efficacy in a malaria mouse model (8). In addition to LysRS, a series of novel bicyclic azetidines demonstrating *in vivo* efficacy were found to specifically target cytosolic phenylalanyl-tRNA synthetase (PheRS) (9), while the potent antimalarials borrelidin and halofuginone inhibit threonyl-tRNA synthetase (ThrRS) (10) and prolyl-tRNA synthetase (ProRS) (11), respectively. Aminoacyl-tRNA synthetases catalyze aminoacylation of tRNAs with their cognate amino acids. *P. falciparum* translation elongation factor 2 (PfeEF2), responsible for the GTP-dependent translocation of the ribosome along mRNA, has also been identified as a promising target (12). Indeed, M5717, a compound specifically targeting PfeEF2, is now undergoing first-in-human trials (13).

The advantage of antimalarials that target core, essential biological processes, such as protein synthesis, is that they have the potential to be effective against multiple life cycle stages of *Plasmodium*. Strategies that can facilitate the identification of protein synthesis inhibitors with diverse modes of action are highly desirable. Previous studies have reported the development of cell-free or *in vitro* translation (IVT) assays capable of identifying antimalarials that target protein synthesis (14–16). Their use has enabled the screening of small libraries as well as validation of the drug mechanism of action (MoA) with respect to protein translation (15). However, these assays have not yet proven suitable or scalable to support high-throughput screening of larger compound libraries. Here, we describe the development of an assay platform devoted to the identification of specific inhibitors of *P. falciparum* translation. This platform is comprised of a *P. falciparum* lysate-based IVT assay that monitors the translation of a luciferase reporter, a counter-screen assay to identify false positives that interfere directly with the luciferase reporter, and an equivalent human IVT assay that is used to guide the identification of selective inhibitors of parasite translation. These 384-well plate assays are capable of identifying a diverse range of translation-specific inhibitors. To demonstrate the power and utility of this platform, pilot screens of the Medicines for Malaria Venture (MMV) open-access Pathogen Box and Pandemic Box compound libraries were carried out, leading to the identification of several novel inhibitors of *P. falciparum* protein synthesis.

RESULTS AND DISCUSSION

Optimization and validation of high-throughput PfIVT and HsIVT assays. Our *P. falciparum* *in vitro* translation (PfIVT) assay is built upon previously established assays (14, 17) and is summarized in Fig. 1A. In this assay, successful reconstitution of *Plasmodium* protein translation is reported via synthesis of a luciferase reporter. For PfIVT, two independent untranslated regions (UTRs), previously shown to promote strong levels of translation (17), were introduced upstream and downstream of the luciferase. The 5' UTR from *P. falciparum* histidine-rich protein 3 (PfHrp3) (18) was

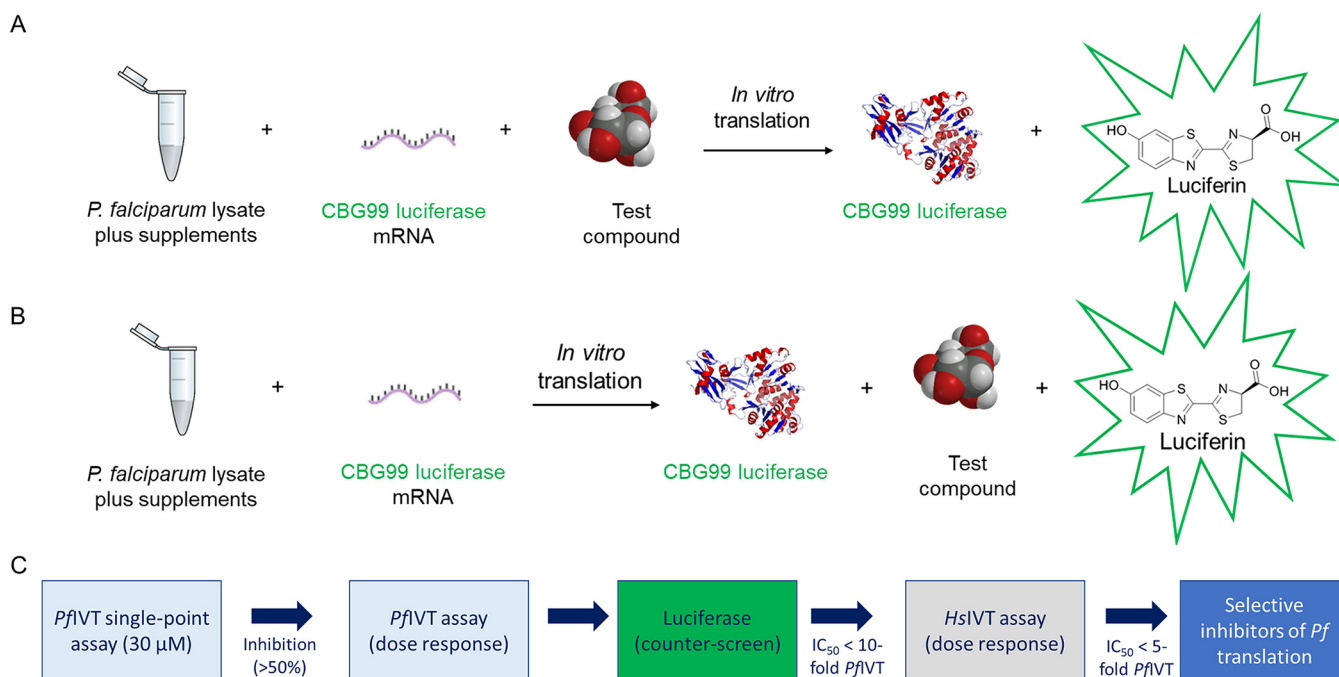


FIG 1 (A and B) Schematic representation of *PfIVT* (A) and luciferase counterscreen (B) assays. (C) Assay workflow and criteria for progression.

introduced upstream of the reporter gene, and the 3' UTR from *P. falciparum* histidine-rich protein 2 (*PfHrp2*) gene (19) was introduced downstream. For the reporter construct to support our complementary human IVT assay (*HsIVT*), the 5' UTR was replaced with an internal ribosome entry site (IRES) from encephalomyocarditis virus (EMCV) (20) and the 3' UTR was replaced with a poly(A) tail (21). It is worth noting that the 5' UTR of EMCV was unable to initiate translation in the *PfIVT* assay and vice versa. Finally, a 30-bp poly(A) tail, present within the vector and downstream of the luciferase gene, was inserted to enhance mRNA stability (21).

Translationally active *P. falciparum* or human embryonic kidney (HEK) 293F lysates were supplemented with accessory, helper, amino acid, and energy regeneration solutions (see Materials and Methods for details). *In vitro* translation reactions were initiated by the addition of purified mRNA to each reaction well. Using this basic assay format, a number of parameters were assessed and optimized, namely, assay temperature, time, mRNA concentration, and reaction volume (summarized in Fig. S2 in the supplemental material). In addition, we compared the luminescence signal of the CBG firefly luciferase with CBG99, derived from the click beetle *Photinus pyralis* (18). Direct comparison of these two luciferases revealed that the luminescence signal for CBG99 was over 2-fold higher than for the original firefly luciferase (Fig. S2), leading us to base our reporter constructs around this superior luciferase. Based on these preliminary studies, the optimal assay parameters were established as reaction volume of 5 μL, assay temperature of 32°C, mRNA concentration of 1,000 ng/μL, and reaction time of 210 min. Under these conditions, the assay reported a signal-to-background ratio of at least 10 and robust *Z'* values above 0.5 in a 384-well plate format.

A selection of established inhibitors of protein translation in *Plasmodium* was then used to validate the *PfIVT* assay, including cycloheximide (inhibitor of the translocation step in the elongation), emetine (inhibitor of 80S ribosome), borrelidin (inhibitor of ThrRS), halofuginone (inhibitor of ProRS), cladosporin (inhibitor of LysRS), and an analogue of DDD107498/M5717 (inhibitor of eEF2), now in clinical trials for the treatment of malaria (Fig. 2). In addition, an inhibitor that mimics a transition state analogue of LysRS (DDD01712277) was also assessed. These compounds, known to inhibit various aspects of cytosolic protein translation in *Plasmodium*, were successfully identified by

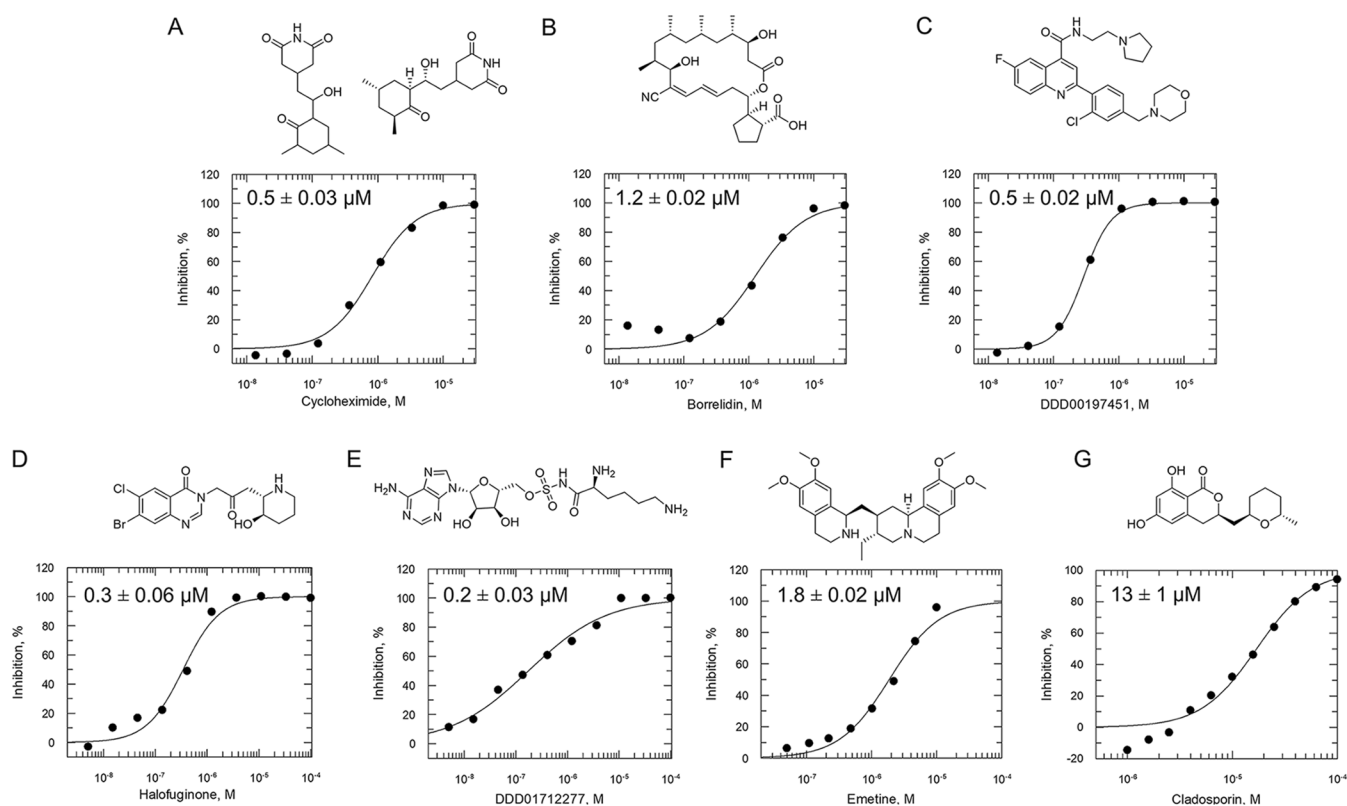


FIG 2 Established inhibitors of translation. Compounds that are known to inhibit different aspects of *in vitro* translation were selected to validate our IVT assay. (A) Cycloheximide is an inhibitor of the translocation step in elongation (46). (B) Borrelidin is an inhibitor of ThrRS (47). (C) DDD00197451 is an inhibitor of translation via eEF2 (44). (D) Halofuginone is an inhibitor of ProRS (11). (E) DDD001712277 is an inhibitor of LysRS. (F) Emetine is an inhibitor of the 80S ribosome (43). (G) Cladosporin is an inhibitor of LysRS (7). All curves shown are from a single technical replicate and are representative of data for at least two biological replicates. IC_{50} values (insets) are weighted means \pm SD from at least two biological replicates.

this assay, validating its ability to identify known translation inhibitors (50% inhibitory concentration [IC_{50}] values summarized in Fig. 2). In contrast, doxycycline and clindamycin, reported to target protein translation within the apicoplast of *P. falciparum* (22, 23), were not active against *Pf*IVT at 100 μM . Collectively, these data illustrate the utility of the *Pf*IVT assay to identify inhibitors of cytoplasmic translation in *P. falciparum* with a broad range of different mechanisms of action. Cycloheximide, emetine, and halofuginone were also used to validate the *Hs*IVT assay and, as expected, were found to successfully inhibit translation in this assay format (Fig. S3), while the *P. falciparum*-specific inhibitor cladosporin was inactive in this assay at 100 μM .

Luciferase counterscreen. To confirm that actives identified in IVT assays are bona fide inhibitors of translation, rather than false positives interfering with the CBG99 luciferase reporter, a counterscreen was established (Fig. 1B). This assay enables the direct inhibition of CBG99 luciferase to be monitored and was validated using luciferase inhibitor I. Using luciferase expressed in IVT reactions, the established luciferase inhibitor I reported an IC_{50} value of 5.5 μM (Fig. S4). Subsequently, false positives were identified as compounds with IC_{50} values less than 1 order of magnitude (10-fold) higher for the *Pf*IVT assay than for the luciferase counterscreen.

Screening of MMV's Pathogen and Pandemic Boxes. The Pathogen Box (<https://www.mmv.org/mmv-open/pathogen-box>) and the Pandemic Box (<https://www.mmv.org/mmv-open/pandemic-response-box>) are collections of 400 diverse, drug-like compounds that have previously demonstrated some level of activity against neglected tropical diseases (NTDs), bacteria, viruses, or fungi. MMV provide these small libraries free of charge to stimulate much-needed drug discovery programs and to take advantage of potential pathogen-hopping opportunities.

Both compound libraries were submitted for assessment in our IVT assay platform (Fig.

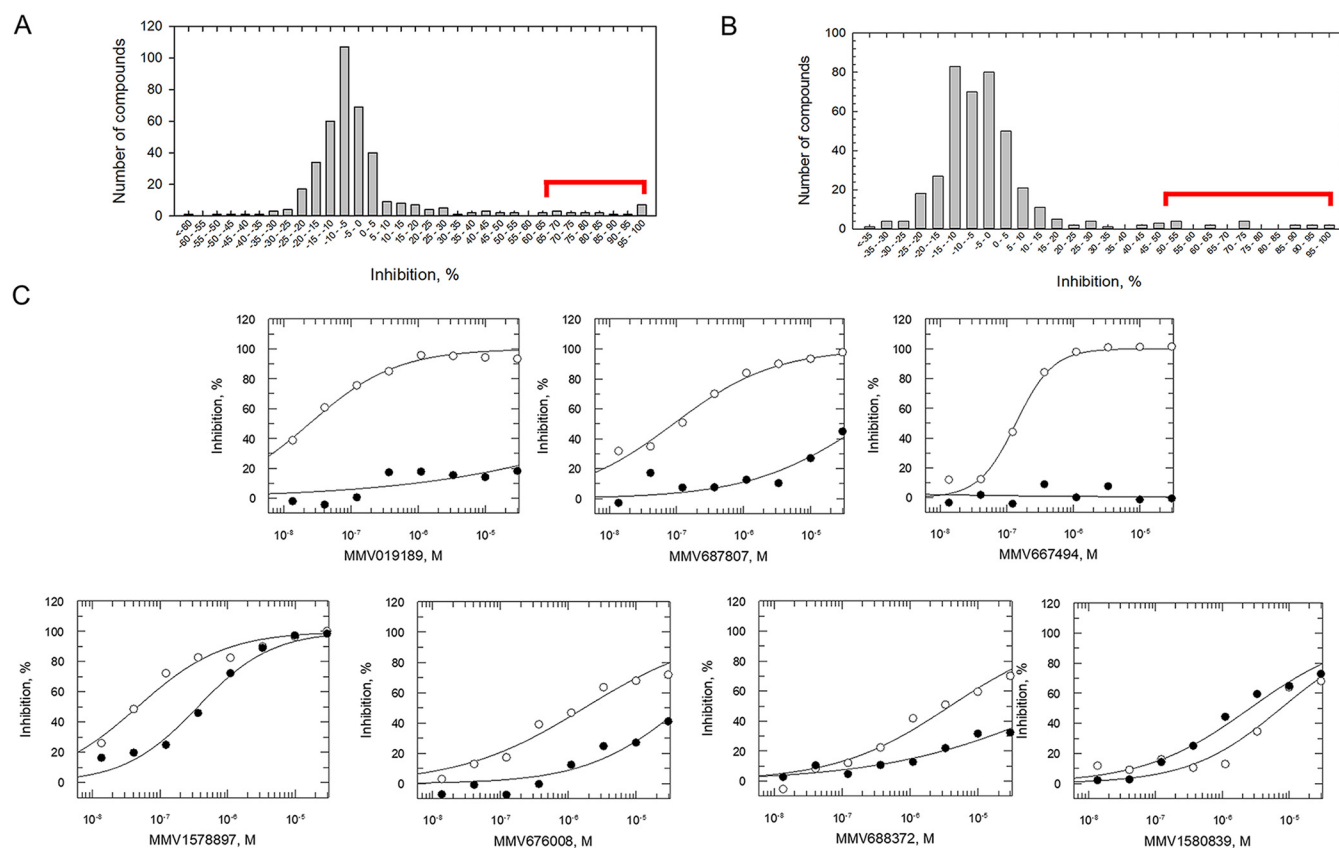


FIG 3 Assessment of the Pathogen Box and the Pandemic Box open access compound libraries against *P. falciparum* IVT assay. (A) Single-point ($30\ \mu\text{M}$) high-throughput screen of the 400 compounds contained within the Pathogen Box against the IVT assay. Compounds demonstrating $>58.02\%$ inhibition were identified as hits (18 compounds; 4.5% hit rate) (highlighted in red). Mean Z' = 0.855. (B) Single-point ($30\ \mu\text{M}$) screen of the Pandemic Box (400 compounds) against *Pf*IVT assay. Compounds demonstrating $>47.29\%$ inhibition were identified as hits (14 compounds; 3.5% hit rate) (highlighted in red). The mean Z' of the assay was 0.825. (C) Assessment of selected hit compounds in 8-point potency assays (closed circles) and a luciferase counterscreen (open circles). All curves shown are from a single technical replicate but representative of data from two biological replicates. IC_{50} values are summarized in Tables 1 and 2.

1C). Initially, compounds were screened in single point ($30\ \mu\text{M}$) against the *Pf*IVT assay. Analysis of our single-point screens revealed normal distributions of inhibition (for the Pathogen Box, the median inhibition $[\bar{x}]$ was 1.00% and the standard deviation $[\sigma]$ was 23.61% [Fig. 3A]; for the Pandemic Box, \bar{x} was 2.08% and σ was 19.75% [Fig. 3B]). DDD00197451, an analogue of eEF2 inhibitor M5717, was added as an internal control in all plates and inhibited $>97\%$ translation (*Pf*IVT), comparable to the positive control cycloheximide. Interestingly, both libraries presented nitazoxanide (MMV688991) among the primary hits, supporting the robustness of *Pf*IVT assay in identifying hits independently. Using a cutoff of 2.5σ (98.7% confidence assuming a normal hit distribution), *Pf*IVT assay identified hit rates of 4.5% for the Pathogen Box (18 compounds demonstrating $>58.02\%$ inhibition) and 3.5% for the Pandemic Box (14 compounds demonstrating $>47.29\%$ inhibition). These represent unusually high hit rates compared to standard target-based screens but were consistent with hit rates seen for high-content and cell-based screens (24). Our interpretation is that since translation is a complex, multicomponent process offering multiple potential targets, the *Pf*IVT assay aligns more closely with phenotype-based screens. It should also be noted that the Pathogen Box contains a number of compounds confirmed to inhibit *P. falciparum* growth *in vitro* (25), which could have positively influenced the hit rate seen in this study.

Primary hits identified in the single-point screen were reassessed in dose-dependent *Pf*IVT assays to confirm their activity and accurately measure their potency. Six primary hits from the Pathogen Box (out of 18) and 4 from the Pandemic Box (out of 14) presented IC_{50} values of $<1\ \mu\text{M}$, with the most potent (nitazoxanide [MMV688991]) returning an IC_{50} value of 20 nM (Table 1). To confirm hits as bona fide inhibitors of *in vitro* translation, rather

TABLE 1 Collated *Pf*IVT and counterscreen data for compounds from MMV's Pathogen Box demonstrating >50% inhibition in a single-point IVT screen at 30 μ M^a

Compound	<i>Pf</i> IVT inhibition at 30 μ M (%)	IC ₅₀ value (μ M)		
		<i>Pf</i> IVT	<i>Hs</i> IVT	Counterscreen
MMV688407	98.7	6 ± 0.09	5.2 ± 0.02	>30
MMV667494	97.7	0.3 ± 0.09	>30	>30
MMV688991	97.0	0.02 ± 0.008	0.04 ± 0.0003	0.02 ± 0.008
MMV688547	96.7	1.8 ± 0.07	2.7 ± 0.02	>30
MMV687807	95.1	0.09 ± 0.007	0.5 ± 0.006	25 ± 0.8
MMV688362	93.5	2.8 ± 0.08	5.6 ± 0.04	>30
MMV634140	88.4	2.9 ± 0.09	>30	>30
MMV019189	84.4	0.03 ± 0.009	7.7 ± 0.3	7 ± 0.6, (>30)
MMV687243	82.5	2.2 ± 0.08	13 ± 0.2	0.9 ± 0.09
MMV637953	78.7	3.1 ± 0.07	>30	>30
MMV688474	78.4	16 ± 0.9	14 ± 0.07	>30
MMV676008	74.9	0.4 ± 0.08	12 ± 0.4	21 ± 0.6
MMV687730	72.4	3.9 ± 0.8	>30	>30
MMV675998	68.9	13 ± 0.9	18 ± 0.13	>30
MMV688271	65.7	18 ± 0.9	13 ± 0.16	>30
MMV676350	65.1	16 ± 0.8	6.7 ± 0.13	>30
MMV687188	64.9	2.4 ± 0.07 (>30)	>30	>30
MMV688372	62.9	0.6 ± 0.06	>30	11 ± 0.8 (>30)
MMV676512	54.2	>30	22 ± 0.46	>30

^aAll IC₅₀ values represent the weighted means ± standard deviations of two technical replicates. Compounds with IC₅₀ values 1 order of magnitude (10-fold) higher for the counterscreen than for the *Pf*IVT assay are considered viable hits and are shaded.

than false positives interfering with the CBG99 luciferase reporter, compounds were next assessed against our validated luciferase counterscreen. False positives were identified as compounds presenting IC₅₀ values <10-fold more potent in the *Pf*IVT assay than in the counterscreen. Using this criterion, two compounds from the Pathogen Box were excluded as false positives: the most potent hit, MMV688991/nitazoxanide, a broad-spectrum anti-infective (26, 27), as well as MMV687243. Thus, 16 compounds from the Pathogen Box were confirmed as inhibitors of *Pf*IVT, with 5 compounds demonstrating submicromolar potency (Table 1). Remarkably, 10 of the 12 hit compounds from the Pandemic Box demonstrated similar IC₅₀ values in the *Pf*IVT and the counterscreen (Table 2), indicating that these are inhibitors of the CBG99 luciferase rather than translation. The remaining two confirmed *Pf*IVT inhibitors (MMV1578897 and MMV1580839) both demonstrated submicromolar potency, with MMV1578897 particularly active (IC₅₀ value, 40 nM).

The 18 confirmed inhibitors of *P. falciparum* translation were assessed in *Hs*IVT assays to detect potential liabilities as inhibitors of human translation. As expected, MMV667494, an analogue of the *Pfe*EF2 inhibitor M5717, was inactive against *Hs*IVT (IC₅₀ value, >30 μ M), in keeping with compounds from this series previously demonstrating a high degree of selective inhibition for *P. falciparum* growth compared to human cells (12). In contrast, the selectivity index for compound MMV687807 inhibiting *Pf*IVT (IC₅₀, 0.09 μ M) compared to *Hs*IVT (IC₅₀, 0.5 μ M) was ≤5-fold, earmarking this compound as potentially a generic inhibitor of translation. Indeed, the established ribosome inhibitor emetine (*Hs*IVT IC₅₀, 1.4 μ M; *Pf*IVT IC₅₀, 0.35 μ M) demonstrated a similarly narrow selectivity window. Combined, these data demonstrate the importance of our *Hs*IVT assay to prioritize primary hits with the potential to specifically inhibit parasite translation.

Prioritization and assessment of hits. A total of 7 compounds were identified as attractive primary hits targeting *P. falciparum* translation. Of these 7, MMV019189 (*Pf*IVT IC₅₀, 0.03 μ M; *Hs*IVT IC₅₀, 7.7 μ M), MMV676008 (*Pf*IVT IC₅₀, 0.4 μ M; *Hs*IVT IC₅₀, 12 μ M), MMV667494 (*Pf*IVT IC₅₀, 0.3 μ M; *Hs*IVT IC₅₀, >30 μ M), and MMV688372 (*Pf*IVT IC₅₀, 0.6 μ M; *Hs*IVT IC₅₀, >30 μ M) demonstrated promising potency against parasite translation, with selectivity windows ≥30-fold over inhibition of translation in human lysate (summarized in Table 1). The remaining 3 compounds—MMV634140 (*Pf*IVT IC₅₀,

TABLE 2 Collated *Pf*AVT and counterscreen data for compounds from MMV's Pandemic Box demonstrating >50% inhibition in a single-point IVT screen at 30 μ M^a

Compound	<i>Pf</i> AVT inhibition at 30 μ M (%)	IC ₅₀ value (μ M)		
		<i>Pf</i> AVT	<i>Hs</i> IVT	Counterscreen
MMV688991	98.3	0.02 \pm 0.007	0.04 \pm 0.0003	0.04 \pm 0.008
MMV002459	87.3	29 \pm 0.9 (>30)	22 \pm 0.3	>30
MMV1578897	93.4	0.04 \pm 0.008	0.18 \pm 0.001	0.4 \pm 0.08
MMV1582495	89.9	0.6 \pm 0.07	3.1 \pm 0.04	1.7 \pm 0.08
MMV1578578	74.6	3.7 \pm 0.07	10 \pm 0.12	1.3 \pm 0.08
MMV1579781	72.4	8.1 \pm 0.09	>30	0.5 \pm 0.08
MMV1580839	73.3	0.8 \pm 0.08	7.6 \pm 0.12	8.3 \pm 0.08
MMV124656	72.6	14 \pm 0.9	17 \pm 0.16	3.8 \pm 0.08
MMV108465	62.6	17 \pm 0.8	23 \pm 0.11	7.6 \pm 0.5
MMV247764	63.2	14 \pm 0.7	23 \pm 0.2	3.2 \pm 0.06
MMV141011	51.8	>30	>30	10 \pm 0.8
MMV003291	52.9	2 \pm 0.07	>30	0.5 \pm 0.08
MMV1634391	52.4	17 \pm 0.6	1.1 \pm 0.01	>30

^aAll IC₅₀ values represent the weighted mean \pm standard deviation of two technical replicates. Compounds with IC₅₀ values 1 order of magnitude (10-fold) higher for the counterscreen compared to the *Pf*AVT assay are considered viable hits and are shaded.

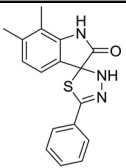
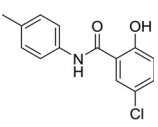
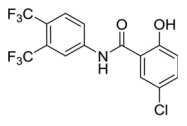
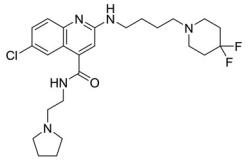
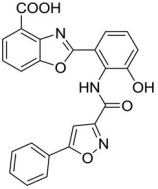
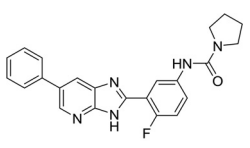
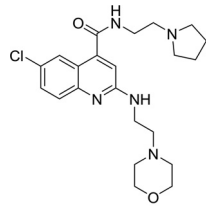
2.9 μ M; *Hs*IVT IC₅₀ >0 μ M), MMV1578897 (*Pf*AVT IC₅₀ 0.04 μ M; *Hs*IVT IC₅₀ 0.18 μ M), and MMV1580839 (*Pf*AVT IC₅₀ 0.8 μ M; *Hs*IVT IC₅₀ 8 μ M)—also showed significant selectivity in the *Pf*AVT assay versus the *Hs*IVT, albeit with more modest safety windows.

We next assessed the potency of the prioritized compounds against asexual-blood-stage (ABS) *P. falciparum* (Table 3). With the exception of MMV676008, all 7 of these compounds demonstrated some level of activity against ABS parasites. Three compounds demonstrated submicromolar activity. MMV667494 and MMV634140, both analogues of the *Pfe*EF2 inhibitor M5717/DDD00107498, were the most potent in ABS assay, with 50% effective concentration (EC₅₀) values of 10 and 41 nM, respectively. MMV019189 also demonstrated promising activity in ABS assays (EC₅₀ 750 nM). In some cases, our prioritized compounds demonstrated higher potency in ABS than in *Pf*AVT assays. Indeed, this was also observed with several established inhibitors of protein translation (Table S1). There are a number of possible explanations for this phenomenon. However, the most likely explanation is that since the potency of competitive inhibitors is dependent on assay conditions, specifically substrate concentrations, the high concentrations of factors such as ATP required to drive the IVT assay may somewhat mask the true potency of inhibitors.

MMV687807 is a potent salicylamide inhibitor of asexual blood and gametocyte stages of *Plasmodium* (*Pf*AVT IC₅₀ 90 nM, EC₅₀ 1.8 μ M). However, this likely generic inhibitor of translation was not prioritized due to its potential liability in human cells (*Hs*IVT IC₅₀ 500 nM). A second salicylanilide derivative, MMV1578897, also showed submicromolar inhibition of *in vitro* translation (*Pf*AVT IC₅₀ 40 nM) but relatively lower activity against blood-stage *P. falciparum*. For these, MMV1578897 and MMV687807 were considered secondary hits that could potentially be used as a backup series in drug discovery programs targeting translation in *Plasmodium*. It is worth noting that these two compounds share the salicylanilide core structure with the antihelminthic drug niclosamide (28). Both compounds have also been reported as having antitubercular activity and were suspected protonophores (29), with MMV1578897 demonstrating broad activity against a range of bacterial pathogens (30).

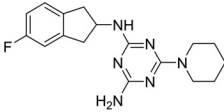
Although showing good potency in *Pf*AVT assay, three other hits were classified as lower-priority compounds since they failed to demonstrate concomitant activity/potency against the *P. falciparum* parasite (Table 3). MMV676008 (*Pf*AVT IC₅₀ 40 nM) is a benzoxazole natural product isolated more than 2 decades ago from cultures of *Streptomyces*; however, it showed an EC₅₀ value of >25 μ M against *P. falciparum in vitro* and thus is not suitable for a hit-to-lead drug discovery program. MMV688372 (*Pf*AVT IC₅₀ 600 nM) is an imidazopyridine previously demonstrating low nanomolar activity against *T. brucei in vitro* and *in vivo* (31). MMV688372 also showed modest

TABLE 3 Structures and antimalarial data for compounds demonstrating sub μM activity in the PfAVT assay

Compound (reference)	Structure	<i>P. falciparum</i> asexual-blood-stage EC_{50} (μM)	PfAVT IC_{50} (μM)
MMV019189 (35)		0.75 ^a	0.03 \pm 0.009
MMV1578897 (30)		5 ^b	0.04 \pm 0.008
MMV687807 (29)		1.8 ^a	0.09 \pm 0.007
MMV667494 (44)		0.010 ^a	0.3 \pm 0.09
MMV676008 (48)		>20 ^a	0.4 \pm 0.08
MMV688372 (31)		13.6	0.6 \pm 0.06
MMV634140 (12)		0.09 ^a	3 \pm 0.09

(Continued on next page)

TABLE 3 (Continued)

Compound (reference)	Structure	<i>P. falciparum</i> asexual-blood-stage EC ₅₀ (μM)	<i>PfAVT</i> IC ₅₀ (μM)
MMV1580839 (34)		5 ^b	0.8 ± 0.08

^aData reported for the *P. falciparum* 3D7 cell line in reference 25.

^bData reported for the *P. falciparum* Dd2 cell line in reference 49.

potency against *P. falciparum* (EC₅₀, 14 μM), though not enough to be prioritized. Interestingly, this compound also shares structural features with two established proteasome inhibitors currently in clinical development for the treatment of visceral leishmaniasis (32, 33). MMV1580839 (*PfAVT* IC₅₀, 900 nM), reported as having an EC₅₀ value of 5 μM against *P. falciparum*, is described as an inhibitor of the bacterial methyltransferases ErmC and ErmAM, blocking the ability of these enzymes to methylate rRNA (34). Finally, the most active confirmed hit in our *PfAVT* assay, MMV019189 (IC₅₀, 30 nM), is a previously reported antimalarial with nanomolar activity against multiple developmental stages of the parasite (35). Undoubtedly, additional work will be required to further define the molecular targets of MMV019189 and other actives described here. One strategy could be to carry out thermal protein profiling (TPP) with compounds using the enriched lysates prepared for our *PfAVT* assay (36, 37). TPP takes advantage of the fact that binding of a ligand to its target can thermally stabilize the target. This approach enables the thermal stability of all proteins within a lysate to be monitored and compared in the presence and absence of test compounds, thus enabling potential targets to be identified. For compounds where structure-activity relationships are better understood, linkers could be attached and used as handles to facilitate the pulldown of targets from IVT lysates and establish molecular targets. Alternatively, parasites resistant to test compounds can be generated through *in vitro* evolution. Whole-genome analysis of resistant clones can lead to the identification of genomic changes pointing to genes encoding compound targets (38). Our ultimate goal will be to structurally enable drug discovery programs focused on evolving more potent or selective analogues of MMV019189 and other promising hit compounds.

Conclusions. In summary, the combination of our IVT assay platform with *in vitro* potency data has led to the identification of one priority hit (MMV019189) and several other compounds of interest that are associated with inhibition of protein synthesis in *P. falciparum* for the first time. These studies clearly demonstrate the power of this assay platform to generate robust data that can be used to prioritize compounds acting via this highly desirable mechanism of action.

MATERIALS AND METHODS

Generation of reporter constructs to support *P. falciparum* and human IVT assays. To support *PfAVT* assays, the production of luciferase mRNA was required. The previously described plasmid pHLH-1, which comprises the 5' UTR of the *P. falciparum* histidine-rich protein 3 (*PfHrp3*) gene upstream of a firefly luciferase reporter gene and the 3' UTR from the histidine-rich protein 2 (*PfHrp2*) gene downstream (19), was used as a starting point. This plasmid was modified to introduce a T7 bacteriophage terminator sequence using site-directed mutagenesis. Briefly, Phusion DNA polymerase (New England Biolabs [NEB]) was used in PCRs in conjunction with a forward (FW; CGC GCT TGG CGA ATC ATG GTC A) and reverse (RV; GCT AGT TAT TGC TCA GCG GCA ATT AAC CCT CAC TAA AGG GAA CAA AAG) primers under the following conditions: 1 × cycle of denaturation at 98°C for 30 s followed by 35 cycles of denaturation at 98°C for 10 s, annealing at 58°C for 15 s, and extension at 72°C for 120 s. The resulting vector (modified pHLH) was linearized with HindIII (NEB), and the PCR-amplified *cbg99* luciferase gene was inserted using Gibson Assembly (NEB). The *cbg99* gene (Fig. S1) was PCR amplified from Promega's pCBG vector using the Phusion DNA polymerase (NEB) and the following primers: FW, ATA TTA ATA CAG TTA TTT TAA AAA AAT GGT GAA GCG TGA GAA AAA TG, and RV, TTT TAA TCT ATT ATT AAA TAA GCT TCT AAC CGC CGG CC. The resulting plasmid (modified pHLH-CBG99) was used in the production of mRNA for the *P. falciparum* IVT assay.

To support the *HsIVT* assay, the pT7CFE vector (Thermo Fisher Scientific), containing an IRES from

the encephalomyocarditis virus (EMCV) and a 30-bp poly(A) region, was digested with MscI and XhoI (NEB). The *cbg99* gene, PCR amplified from the pCBG vector using FW primer GAA AAA CAC GAT GAT AAT ATG GCC ACC ATG GTG AAG CGT GAG AAA AAT G and RV primer CAG TGG TGG TGG TGG TGG TGC TCG AGA CCG CCG GC, encompassing homology to pT7CFE. The PCR product was then cloned into the digested pT7CFE vector using Gibson Assembly (NEB). The resulting plasmid (pT7CFE-CBG99) was used in the production of mRNA for the human IVT assay.

Assay validation construct. In preliminary assay development experiments, a plasmid that facilitated expression of a hemagglutinin (HA)-tagged version of the firefly luciferase (Fig. S1) was used. In this study, the modified pHLH-1 plasmid, described above, was used as a starting point. The plasmid was digested with NsiI and HindIII (NEB) to release the Cbg luciferase. A Genestring (Life Technologies) containing homology to the digested plasmid was cloned using Gibson Assembly inserting a 3×HA tag and tobacco etch virus (TEV) cleavage site into the vector (Fig. S1). This formed a universal vector (pHLHUNI) that could be used to insert genes of interest fused to an N- or C-terminal 3×HA tag and TEV cleavage site. The newly formed vector was linearized with HindIII and the firefly luciferase (*luc*) gene inserted, again using Gibson Assembly.

Western blotting. Proteins were separated on 12% SDS-PAGE gels and then transferred to nitrocellulose membranes using an iBlot 2 (Thermo Fisher) system as per the manufacturer's instructions. The membrane was blocked in 10% (wt/vol) milk in phosphate-buffered saline (PBS) containing 0.1% Tween 20 (PBS-T) for 1 h. Following blocking, the membrane was incubated in 2% (wt/vol) milk in PBS-T containing the HA tag-specific primary antibody 12CA5 (Cell Signaling) at a dilution of 1:1,000 for 1 h. The membrane was then washed with PBS-T (three times for 5 min). Following a washing, membranes were incubated in 2% milk in PBS-T containing an anti-rabbit secondary antibody conjugated to horseradish peroxidase (HRP; Merck) at a dilution of 1:5,000 for 1 h prior to washing in PBS-T (three times for 5 min). HA-tagged protein on the membrane was detected using the ECL Western blot detection reagent (GE Healthcare) as per the manufacturer's instructions and visualized using a Gel Doc XR+ imaging system (Bio-Rad).

In vitro transcription of mRNA. Reactions to produce *cbg99* mRNA were run using 40 mM HEPES (pH 7.4), 18 mM magnesium acetate, ribonucleotide triphosphates (5 mM each), 2 mM spermidine, 40 mM dithiothreitol (DTT), 0.0025 U/ μ L inorganic pyrophosphatase, modified pHLH-CBG99 for the parasite assay and pT7CFE-CBG99 for the human assay (70 ng/ μ L), RNase inhibitor (3 U/ μ L), and T7 RNA polymerase (10 U/ μ L). This reaction mixture was incubated for 100 min at 37°C, and DNase I (0.1 mg/mL) was added for the final 20 min of the incubation. The reaction mixture was then diluted 1:1 with RNase-free H₂O and RNA was precipitated using 1.6 M (final concentration) lithium chloride, followed by incubation on ice (30 min) and centrifugation (15,000 × *g*, 20 min, 4°C). The resulting pellet was dissolved in 270 μ L RNase-free H₂O with agitation at 30°C. RNA was precipitated once again by addition of 3 M ammonium acetate (30 μ L) and ice-cold absolute ethanol (700 μ L). Samples were incubated at –20°C for 30 min, and mRNA was precipitated by centrifugation (15,000 × *g*, 20 min, 4°C). The supernatant was removed and discarded, and the pellet was rinsed twice with 70% ethanol. Residual ethanol was removed, and the pellet was air dried (1 h) prior to solubilization with RNase-free water. The concentration of the resuspended RNA was determined using a NanoDrop spectrophotometer.

Parasite strain and culture conditions. The *Plasmodium falciparum* reference strain 3D7 used throughout this study was cultured as previously described (39). Briefly, cultures incubated at 37°C in a humidified atmosphere of 1% O₂ and 3% CO₂ in balance with N₂ were maintained in RPMI 1640 media supplemented with 5% A⁺ human red blood cells (provided by the Scottish National Blood Transfusion Service), 25 mM HEPES, 2 mM L-glutamine, 0.5% AlbuMAX II (Gibco), 12 mM sodium bicarbonate, 0.2 mM hypoxanthine, and 20 mg/L gentamicin (pH 7.3).

P. falciparum lysate preparation. 3D7 parasites were synchronized following two rounds of treatment with D-sorbitol (5%), as previously described (40). The hematocrit was reduced from 5% (for standard culture) to 1.5 to 2% and cultures were transferred into HYPERflasks (Corning). Fresh medium was added once or twice daily. Late trophozoite/schizont stage parasites were harvested by centrifugation (1,800 × *g*, 15 min, 4°C, low brake) once parasitemia reached 8 to 15%. Harvested red blood cells (infected) were lysed by incubation in 0.1% (wt/vol) saponin on ice for 10 min with gentle agitation. Free parasites were harvested by centrifugation (2,800 × *g*, 10 min, 4°C) and washed 3 times in wash buffer (WB; 100 mM potassium acetate, 2.5 mM magnesium acetate, 45 mM HEPES [pH 7.4], 250 mM sucrose, 2 mM dithiothreitol, and 15 μ M leupeptin) to remove lysed red blood cell debris. The resulting pellet was resuspended in 1 volume of WB supplemented with cOmplete EDTA-free protease inhibitor cocktail (Roche; 1 tablet/20 mL) and human RNase A inhibitor (Sigma; 5 U/mL). Parasite lysis was achieved by nitrogen cavitation using a prechilled 45-mL Parr cell disruption vessel (1,500 lb/in², 60 min, 4°C). To clarify the lysate, it was centrifuged (10,000 × *g*, 15 min, 4°C), and the supernatant was collected, transferred into fresh tubes, and centrifuged (30,000 × *g*, 15 min, 4°C). As a quality assurance step for each lysate, the RNA content of the resulting supernatant was determined using a NanoDrop spectrophotometer (Shimadzu). Supernatants with RNA levels of >250 ng/ μ L were aliquoted (100 μ L), flash frozen in liquid nitrogen, and stored at –80°C.

HEK 293F cell culture. FreeStyle human embryonic kidney (HEK) 293F cells (Thermo Fisher Scientific) were grown in 500-mL polycarbonate Erlenmeyer vented flasks (Corning) containing FreeStyle 293 expression medium (Life Technologies) upon reaching a density of approximately 2 × 10⁶. Cells were then centrifuged at 1,000 × *g* for 10 min at 4°C, the medium was discarded, and the resulting pellet was washed once in buffer II containing 20 U of human placental RNase inhibitor (Sigma-Aldrich) and cOmplete EDTA-free inhibitor cocktail (Roche) before being centrifuged at 2,800 × *g* for 10 min. Clarified HEK cell lysate was obtained in the same way as described for *P. falciparum* lysate.

P. falciparum and human IVT assays. *Pf*IVT and *Hs*IVT reactions (5 μ L final volume) were performed in 384-well plates (Corning) containing 50% lysate from cells (either *P. falciparum* or HEK 293F), 10% amino acid solution (final concentration of 400 μ M for each amino acid in 60 mM KOH; biotech rabbit), 10% energy recovery solution (final assay concentrations of 40 mM HEPES [pH 7.4], 1.5 mM ATP, 0.15 mM GTP, 40 U/mL creatine phosphate, and 40 U/mL creatine phosphokinase), 10% helper solution (final assay concentrations of 200 μ M cystine, 2% polyethylene glycol 3000 [PEG 3000]), 1 mM spermidine, 0.5 mM folinic acid, and 15 μ M leupeptin), 10% supplemental salt solution (22.5 mM HEPES [pH 7.4], 50 mM potassium acetate, 1 mM magnesium acetate, 1 mM DTT, 1 U/mL human placental RNase inhibitor, 0.1 mM leupeptin), and 10% *cbg99* luciferase mRNA (3,000 ng/mL). A master mix solution containing all components was prepared on ice prior to assays, and 5 μ L was dispensed into wells using an automated Integra VIAFLO 16-channel 12.5- μ L pipette. Assays were incubated for 210 min at 32°C, and luciferase buffer (5 μ L; final assay concentrations of 45 mM HEPES [pH 7.4], 1 mM MgCl₂, 1 mM ATP, 5 mM DTT, 1% Triton X-100, 10 mg/mL bovine serum albumin [BSA], 1 mg/mL D-luciferin, and 1 \times Pierce firefly signal enhancer) was added to read luminescence using a BMG PheraStar plate reader. Cycloheximide was used as a positive control in both *Pf*IVT and *Hs*IVT reactions, representing 100% inhibition. Hits were assessed as inhibitors of translation in both IVT assays in 8-point dose-dependent assays (30 μ M to 13.7 nM; 1:3 dilutions). Relative activity of luciferase was calculated based on positive-control reactions.

False-positive counterscreen. Hits identified in our primary assay screen were assessed for their potential to interfere with the *cbg99* luciferase reporter. For this counterscreen, the master mix containing all the components required for translation (as described above) was incubated for 210 min at 32°C, resulting in the *in vitro* translation of *cbg99* luciferase. The produced luciferase was then incubated with test compounds for 5 min prior to the addition of luciferase reaction buffer. Luciferase I inhibitor (Calbiochem) was used at 50 μ M as a positive control in each assay, representing 100% inhibition. Hits from the primary screen were assessed as luciferase inhibitors in 8-point dose-dependent assays ranging from 30 μ M to 13.7 nM (1:3 dilutions). Levels of luciferase inhibition were determined relative to the positive control.

Inhibitor studies. Test compounds (10 mM in 100% dimethyl sulfoxide [DMSO]) were dispensed into 384-well assay plates using the acoustic Echo 550 dispenser (Labcyte). Compound libraries were screened at a single inhibitor concentration (30 μ M), and compounds inhibiting >50% *Pf*IVT activity were selected for dose-dependent analysis. For dose-response assays, compound concentrations ranging from 30 μ M to 13.7 nM (1:3 dilutions) were assessed in 8-point inhibition assays. IC₅₀ values were determined using XLFit using a 4-parameter equation. Cycloheximide (50 μ M) was used as a positive control for *Pf*IVT on every assay plate representing 100% inhibition.

Compounds and libraries. Established inhibitors of IVT—cycloheximide (41), borrelidin (42), halofuginone (11), and emetine (43)—were purchased from Sigma. Open-access compound libraries Pathogen Box and the Pandemic Response Box, both 400-compound libraries, were kindly provided by Medicines for Malaria Venture (MMV). DDD00197451 (44) and DDD01712277 (12) were synthesized as previously described. Cladosporin was kindly provided by Chris Walpole from the Structural Genomics Consortium.

Quality control of library compounds. Hits identified in our primary assay screen were subjected to mass spectrometry to confirm purity and compound identity. For this, library compounds in DMSO were diluted 20-fold in a clean, u-shaped, deep-well 384-well plate. The plate was heat sealed (Waters heat sealer) and vortexed. Samples were then injected into an ultrahigh-performance liquid chromatography (UHPLC)-mass spectrometry (MS) 2020 single-quadrupole mass spectrometer with atmospheric pressure chemical ionization and electrospray ionization (ESI) probes fitted (DG-20A3R and DG-20A5R degasser; 2 \times LC-30 AD binary pumps; SIL-30AC MP multiplate autosampler with sample chiller; CTO-20AC plus 2 column switching valve; SPD-M30A UV/visible diode array detector with 1-cm flow cell). Library compounds (2 μ L) were injected into a Hypersil Gold column (Thermo Fisher Scientific; 1.9- μ m internal diameter, 50-mm length, 175-Å pore size) and HPLC separated using a gradient of solvent A (water/0.05% formic acid) and solvent B (acetonitrile/0.05% formic acid) at 0.6 mL/min and 50°C. Detection was performed at 254 nm (40°C) using a mass spectral range from 50 to 1,000 Da (both positive and negative modes; scan speed, 15,000 Da/s; interface voltage, 4.5 kV). Shimadzu LabSystems 5.91 software was used to control sample injections into the LC-MS system and to analyze processed data (integration of peak areas and assessment of masses). Trazodone hydrochloride and reserpine were used as internal standards.

SYBR green-based P. falciparum growth inhibition assay. Our SYBR green asexual-growth assay was based on a previous report (45). In brief, 96-well black clear-bottom plates (Corning) were pre-printed with a compound and normalized with DMSO to 0.5% of a total assay volume of 100 μ L. Highly synchronized ring-stage parasites and blood were added to a 2% final parasitemia and 1% hematocrit. The compounds were incubated with parasites for 72 h prior to freezing at -20°C (to aid cell lysis). The plate was thawed on ice and lysis buffer (20 mM Tris pH 7.5, 5 mM EDTA, 0.008% [w/v] saponin, 0.08% [v/v]) containing SYBR green I (Thermo Fisher Scientific) at a final concentration of 0.02% (v/v) was added. The 96-well plate was equilibrated to room temperature for 1 h before fluorescence was determined on a TECAN Infinite Pro 200 microplate reader using green fluorescent protein (GFP) filters (excitation, 485 nm; emission, 535 nm). Data were fitted to a two-parameter equation using GraFit version 7.0 (Erithacus Software), and EC₅₀ values were calculated. An excess of the standard inhibitor mefloquine (10 μ M) was used to define 0% parasite growth.

SUPPLEMENTAL MATERIAL

Supplemental material is available online only.

SUPPLEMENTAL FILE 1, PDF file, 0.3 MB.

ACKNOWLEDGMENTS

This work was supported by funding from MMV (RD-09-0043). We acknowledge the support of our MMV liaison Didier Leroy. Fabio Tamaki and Fabio Fisher contributed to this work equally. Fabio Tamaki optimised the assay for use in 384-well format while Fabio Fisher carried out initial assay development. We would like to acknowledge the assistance of the DDU's Compound Management team in this study. In addition, we would like to acknowledge advice from Manu De Rycker, DDU. The Wellcome Centre for Anti-Infectives Research acknowledges support from the Wellcome Trust (203134/Z/16/Z). J.B. was supported by an Investigator Award from Wellcome (100993/Z/13/Z). This work was supported via funding from Wellcome (Pathfinder Award to J.B.) (105686/Z/14/Z) and a Medical Research Council, UK, Confidence in Concept Award to J.B. (P51477).

REFERENCES

- World Health Organization. 2019. World malaria report 2019. World Health Organization, Geneva, Switzerland.
- Menard D, Dondorp A. 2017. Antimalarial drug resistance: a threat to malaria elimination. *Cold Spring Harb Perspect Med* 7:a025619. <https://doi.org/10.1101/cshperspect.a025619>.
- Ross LS, Fidock DA. 2019. Elucidating mechanisms of drug-resistant Plasmodium falciparum. *Cell Host Microbe* 26:35–47. <https://doi.org/10.1016/j.chom.2019.06.001>.
- World Health Organization. 2015. Guidelines for the treatment of malaria, 3rd ed. World Health Organization, Geneva, Switzerland.
- Woodrow CJ, White NJ. 2017. The clinical impact of artemisinin resistance in Southeast Asia and the potential for future spread. *FEMS Microbiol Rev* 41:34–48. <https://doi.org/10.1093/femsre/fuw037>.
- Uwimana A, Legrand E, Stokes BH, Ndikumana JM, Warsame M, Umulisa N, Ngamije D, Munyaneza T, Mazarati JB, Munguti K, Campagne P, Criscuolo A, Arief F, Murindahabi M, Ringwald P, Fidock DA, Mbituyumuremyi A, Menard D. 2020. Emergence and clonal expansion of in vitro artemisinin-resistant Plasmodium falciparum kelch13 R561H mutant parasites in Rwanda. *Nat Med* 26:1602–1608. <https://doi.org/10.1038/s41591-020-1005-2>.
- Hoepfner D, McNamara CW, Lim CS, Studer C, Riedl R, Aust T, McCormack SL, Plouffe DM, Meister S, Schuierer S, Plikat U, Hartmann N, Staedtler F, Costea S, Schmitt EK, Petersen F, Supek F, Glynn RJ, Tallarico JA, Porter JA, Fishman MC, Bodenreider C, Diagana TT, Movva NR, Winzeler EA. 2012. Selective and specific inhibition of the Plasmodium falciparum lysyl-tRNA synthetase by the fungal secondary metabolite cladosporin. *Cell Host Microbe* 11:654–663. <https://doi.org/10.1016/j.chom.2012.04.015>.
- Baragaña B, Forte B, Choi R, Nakazawa Hewitt S, Bueren-Calabuig JA, Pisco JP, Peet C, Dranow DM, Robinson DA, Jansen C, Norcross NR, Vinayak S, Anderson M, Brooks CF, Cooper CA, Damerow S, Delves M, Dowers K, Duffy J, Edwards TE, Hallyburton I, Horst BG, Hulverson MA, Ferguson L, Jiménez-Díaz MB, Jumaní RS, Lorimer DD, Love MS, Maher S, Matthews H, McNamara CW, Miller P, O'Neill S, Ojo KK, Osuna-Cabello M, Pinto E, Post J, Riley J, Rottmann M, Sanz LM, Scullion P, Sharma A, Shepherd SM, Shishikura Y, Simeons FRC, Stebbins EE, Stojanovski L, Straschil U, Tamaki FK, Tamjar J, et al. 2019. Lysyl-tRNA synthetase as a drug target in malaria and cryptosporidiosis. *Proc Natl Acad Sci U S A* 116:7015–7020. <https://doi.org/10.1073/pnas.1814685116>.
- Kato N, Comer E, Sakata-Kato T, Sharma A, Sharma M, Maetani M, Bastien J, Brancucci NM, Bittker JA, Corey V, Clarke D, Derbyshire ER, Dornan GL, Duffy S, Eckley S, Itoe MA, Koolen KM, Lewis TA, Lui PS, Lukens AK, Lund E, March S, Meibalan E, Meier BC, McPhail JA, Mitasev B, Moss EL, Sayes M, Van Gessel Y, Wawer MJ, Yoshinaga T, Zeeman AM, Avery VM, Bhatia SN, Burke JE, Catteruccia F, Clardy JC, Clemons PA, Decherer KJ, Duvall JR, Foley MA, Gusovsky F, Kocken CH, Marti M, Morningstar ML, Munoz B, Neafsey DE, Sharma A, Winzeler EA, Wirth DF, Scherer CA, Schreiber SL. 2016. Diversity-oriented synthesis yields novel multistage antimalarial inhibitors. *Nature* 538:344–349. <https://doi.org/10.1038/nature19804>.
- Novoa EM, Camacho N, Tor A, Wilkinson B, Moss S, Marín-García P, Azcárate IG, Bautista JM, Mirando AC, Francklyn CS, Varon S, Royo M, Cortés A, Ribas de Pouplana L. 2014. Analogs of natural aminoacyl-tRNA synthetase inhibitors clear malaria in vivo. *Proc Natl Acad Sci U S A* 111:E5508–E5517. <https://doi.org/10.1073/pnas.1405994111>.
- Keller TL, Zocco D, Sundrud MS, Hendrick M, Edenius M, Yum J, Kim YJ, Lee HK, Cortese JF, Wirth DF, Dignam JD, Rao A, Yeo CY, Mazitschek R, Whitman M. 2012. Halofuginone and other febrifugine derivatives inhibit prolyl-tRNA synthetase. *Nat Chem Biol* 8:311–317. <https://doi.org/10.1038/nchembio.790>.
- Baragaña B, Hallyburton I, Lee MC, Norcross NR, Grimaldi R, Otto TD, Proto WR, Blagborough AM, Meister S, Wirjanata G, Ruecker A, Upton LM, Abraham TS, Almeida MJ, Pradhan A, Porzelle A, Luksch T, Martínez MS, Luksch T, Bolscher JM, Woodland A, Norval S, Zuccotto F, Thomas J, Simeons F, Stojanovski L, Osuna-Cabello M, Brock PM, Churcher TS, Sala KA, Zakutansky SE, Jiménez-Díaz MB, Sanz LM, Riley J, Basak R, Campbell M, Avery VM, Sauerwein RW, Decherer KJ, Noviyanti R, Campo B, Frearson JA, Angulo-Barturen I, Ferrer-Bazaga S, Gamo FJ, Wyatt PG, Leroy D, Siegl P, Delves MJ, Kyle DE, et al. 2015. A novel multiple-stage antimalarial agent that inhibits protein synthesis. *Nature* 522:315–320. <https://doi.org/10.1038/nature14451>.
- McCarthy JS, Yalkinoglu Ö, Odedra A, Webster R, Oeuvray C, Tappert A, Bezuidenhout D, Giddins MJ, Dhingra SK, Fidock DA, Marquart L, Webb L, Yin X, Khandelwal A, Bagchus WM. 2021. Safety, pharmacokinetics, and antimalarial activity of the novel plasmodium eukaryotic translation elongation factor 2 inhibitor M5717: a first-in-human, randomized, placebo-controlled, double-blind, single ascending dose study and volunteer infection study. *Lancet Infect Dis* 21:1713–1724. [https://doi.org/10.1016/S1473-3099\(21\)00252-8](https://doi.org/10.1016/S1473-3099(21)00252-8).
- Ahyong V, Sheridan CM, Leon KE, Witchley JN, Diep J, DeRisi JL. 2016. Identification of Plasmodium falciparum specific translation inhibitors from the MMV Malaria Box using a high throughput in vitro translation screen. *Malar J* 15:173. <https://doi.org/10.1186/s12936-016-1231-8>.
- Sheridan CM, Garcia VE, Ahyong V, DeRisi JL. 2018. The Plasmodium falciparum cytoplasmic translation apparatus: a promising therapeutic target not yet exploited by clinically approved anti-malarials. *Malar J* 17:465. <https://doi.org/10.1186/s12936-018-2616-7>.
- Ferreras A, Triana L, Correia H, Sánchez E, Herrera F. 2000. An in vitro system from Plasmodium falciparum active in endogenous mRNA translation. *Mem Inst Oswaldo Cruz* 95:231–235. <https://doi.org/10.1590/S0074-0276200000200017>.
- Baumann H, Matthews H, Li M, Hu JJ, Willison KR, Baum J. 2018. A high throughput in vitro translation screen towards discovery of novel antimalarial protein translation inhibitors. *bioRxiv* <https://doi.org/10.1101/248740>.
- Wood KV, Lam YA, Seliger HH, McElroy WD. 1989. Complementary DNA coding click beetle luciferases can elicit bioluminescence of different colors. *Science* 244:700–702. <https://doi.org/10.1126/science.2655091>.
- Wu Y, Sifri CD, Lei HH, Su XZ, Wellem TE. 1995. Transfection of Plasmodium falciparum within human red blood cells. *Proc Natl Acad Sci U S A* 92:973–977. <https://doi.org/10.1073/pnas.92.4.973>.
- Wong ET, Ngoi SM, Lee CG. 2002. Improved co-expression of multiple genes in vectors containing internal ribosome entry sites (IRESes) from human genes. *Gene Ther* 9:337–344. <https://doi.org/10.1038/sj.gt.3301667>.
- Gallie DR. 1991. The cap and poly(A) tail function synergistically to regulate mRNA translational efficiency. *Genes Dev* 5:2108–2116. <https://doi.org/10.1101/gad.5.11.2108>.
- Okada M, Guo P, Nalder SA, Sigala PA. 2020. Doxycycline has distinct apicoplast-specific mechanisms of antimalarial activity. *Elife* 9:e60246. <https://doi.org/10.7554/eLife.60246>.

23. Dahl EL, Rosenthal PJ. 2008. Apicoplast translation, transcription and genome replication: targets for antimalarial antibiotics. *Trends Parasitol* 24: 279–284. <https://doi.org/10.1016/j.pt.2008.03.007>.
24. Roy A. 2018. Early probe and drug discovery in academia: a minireview. *High Throughput* 7:4. <https://doi.org/10.3390/ht7010004>.
25. Duffy S, Sykes ML, Jones AJ, Shelper TB, Simpson M, Lang R, Poulsen SA, Sleebs BE, Avery VM. 2017. Screening the Medicines for Malaria Venture Pathogen Box across multiple pathogens reclassifies starting points for open-source drug discovery. *Antimicrob Agents Chemother* 61:e00379-17. <https://doi.org/10.1128/AAC.00379-17>.
26. Rossignol JF. 2014. Nitazoxanide: a first-in-class broad-spectrum antiviral agent. *Antiviral Res* 110:94–103. <https://doi.org/10.1016/j.antiviral.2014.07.014>.
27. Adagu IS, Nolder D, Warhurst DC, Rossignol JF. 2002. In vitro activity of nitazoxanide and related compounds against isolates of *Giardia intestinalis*, *Entamoeba histolytica* and *Trichomonas vaginalis*. *J Antimicrob Chemother* 49:103–111. <https://doi.org/10.1093/jac/49.1.103>.
28. Weinbach EC, Garbus J. 1969. Mechanism of action of reagents that uncouple oxidative phosphorylation. *Nature* 221:1016–1018. <https://doi.org/10.1038/2211016a0>.
29. Lee IY, Gruber TD, Samuels A, Yun M, Nam B, Kang M, Crowley K, Winterroth B, Boshoff HI, Barry CE, III. 2013. Structure-activity relationships of antitubercular salicylanilides consistent with disruption of the proton gradient via proton shuttling. *Bioorg Med Chem* 21:114–126. <https://doi.org/10.1016/j.bmc.2012.10.056>.
30. Pauk K, Zdražilová I, Imramovský A, Vinšová J, Pokorná M, Masaříková M, Cízek A, Jampílek J. 2013. New derivatives of salicylamides: preparation and antimicrobial activity against various bacterial species. *Bioorg Med Chem* 21:6574–6581. <https://doi.org/10.1016/j.bmc.2013.08.029>.
31. Tatipaka HB, Gillespie JR, Chatterjee AK, Norcross NR, Hulverson MA, Ranade RM, Nagendar P, Creason SA, McQueen J, Duster NA, Nagle A, Supek F, Molteni V, Wenzler T, Brun R, Glynne R, Buckner FS, Gelb MH. 2014. Substituted 2-phenylimidazopyridines: a new class of drug leads for human African trypanosomiasis. *J Med Chem* 57:828–835. <https://doi.org/10.1021/jm401178t>.
32. Wyllie S, Brand S, Thomas M, De Rycker M, Chung CW, Pena I, Bingham RP, Bueren-Calabuig JA, Cantizani J, Cebrian D, Craggs PD, Ferguson L, Goswami P, Hobrath J, Howe J, Jeacock L, Ko EJ, Korczynska J, MacLean L, Manthri S, Martinez MS, Mata-Cantero L, Moniz S, Nühs A, Osuna-Cabello M, Pinto E, Riley J, Robinson S, Rowland P, Simeons FRC, Shishikura Y, Spinks D, Stojanovski L, Thomas J, Thompson S, Viayna Gaza E, Wall RJ, Zuccotto F, Horn D, Ferguson MAJ, Fairlamb AH, Fiandor JM, Martin J, Gray DW, Miles TJ, Gilbert IH, Read KD, Marco M, Wyatt PG. 2019. Preclinical candidate for the treatment of visceral leishmaniasis that acts through proteasome inhibition. *Proc Natl Acad Sci U S A* 116:9318–9323. <https://doi.org/10.1073/pnas.1820175116>.
33. Khare S, Nagle AS, Biggart A, Lai YH, Liang F, Davis LC, Barnes SW, Mathison CJ, Myburgh E, Gao MY, Gillespie JR, Liu X, Tan JL, Stinson M, Rivera IC, Ballard J, Yeh V, Groessl T, Federe G, Koh HX, Venable JD, Bursulaya B, Shapiro M, Mishra PK, Spraggon G, Brock A, Mottram JC, Buckner FS, Rao SP, Wen BG, Walker JR, Tuntland T, Molteni V, Glynne RJ, Supek F. 2016. Proteasome inhibition for treatment of leishmaniasis, Chagas disease and sleeping sickness. *Nature* 537:229–233. <https://doi.org/10.1038/nature19339>.
34. Hajduk PJ, Dinges J, Schkeryantz JM, Janowick D, Kaminski M, Tufano M, Augeri DJ, Petros A, Nienaber V, Zhong P, Hammond R, Coen M, Beutel B, Katz L, Fesik SW. 1999. Novel inhibitors of Erm methyltransferases from NMR and parallel synthesis. *J Med Chem* 42:3852–3859. <https://doi.org/10.1021/jm990293a>.
35. Gamo FJ, Sanz LM, Vidal J, de Cozar C, Alvarez E, Lavandera JL, Vanderwall DE, Green DV, Kumar V, Hasan S, Brown JR, Peishoff CE, Cardon LR, Garcia-Bustos JF. 2010. Thousands of chemical starting points for antimalarial lead identification. *Nature* 465:305–310. <https://doi.org/10.1038/nature09107>.
36. Corpas-Lopez V, Moniz S, Thomas M, Wall RJ, Torrie LS, Zander-Dinse D, Tinti M, Brand S, Stojanovski L, Manthri S, Hallyburton I, Zuccotto F, Wyatt PG, De Rycker M, Horn D, Ferguson MAJ, Clos J, Read KD, Fairlamb AH, Gilbert IH, Wyllie S. 2019. Pharmacological validation of N-myristoyltransferase as a drug target in *Leishmania donovani*. *ACS Infect Dis* 5:111–122. <https://doi.org/10.1021/acsinfecdis.8b00226>.
37. Dziekan JM, Wirjanata G, Dai L, Go KD, Yu H, Lim YT, Chen L, Wang LC, Puspita B, Prabhu N, Sobota RM, Nordlund P, Bozdech Z. 2020. Cellular thermal shift assay for the identification of drug-target interactions in the *Plasmodium falciparum* proteome. *Nat Protoc* 15:1881–1921. <https://doi.org/10.1038/s41596-020-0310-z>.
38. Carolino K, Winzeler EA. 2020. The antimalarial resistome—finding new drug targets and their modes of action. *Curr Opin Microbiol* 57:49–55. <https://doi.org/10.1016/j.mib.2020.06.004>.
39. Trager W, Jensen JB. 1976. Human malaria parasites in continuous culture. *Science* 193:673–675. <https://doi.org/10.1126/science.781840>.
40. Lambros C, Vanderberg JP. 1979. Synchronization of *Plasmodium falciparum* erythrocytic stages in culture. *J Parasitol* 65:418–420. <https://doi.org/10.2307/3280287>.
41. Kerridge D. 1958. The effect of actidione and other antifungal agents on nucleic acid and protein synthesis in *Saccharomyces carlsbergensis*. *J Gen Microbiol* 19:497–506. <https://doi.org/10.1099/00221287-19-3-497>.
42. Gao YM, Wang XJ, Zhang J, Li M, Liu CX, An J, Jiang L, Xiang WS. 2012. Borrelidin, a potent antifungal agent: insight into the antifungal mechanism against *Phytophthora sojae*. *J Agric Food Chem* 60:9874–9881. <https://doi.org/10.1021/jf302857x>.
43. Wong W, Bai XC, Brown A, Fernandez IS, Hanssen E, Condrón M, Tan YH, Baum J, Scheres SH. 2014. Cryo-EM structure of the *Plasmodium falciparum* 80S ribosome bound to the anti-protozoan drug emetine. *Elife* 3:e03080. <https://doi.org/10.7554/eLife.03080>.
44. Baragaña B, Norcross NR, Wilson C, Porzelle A, Hallyburton I, Grimaldi R, Osuna-Cabello M, Norval S, Riley J, Stojanovski L, Simeons FR, Wyatt PG, Delves MJ, Meister S, Duffy S, Avery VM, Winzeler EA, Sinden RE, Wittlin S, Frearson JA, Gray DW, Fairlamb AH, Waterson D, Campbell SF, Willis P, Read KD, Gilbert IH. 2016. Discovery of a quinoline-4-carboxamide derivative with a novel mechanism of action, multistage antimalarial activity, and potent in vivo efficacy. *J Med Chem* 59:9672–9685. <https://doi.org/10.1021/acs.jmedchem.6b00723>.
45. Matthews H, Deakin J, Rajab M, Idris-Usman M, Nirmalan NJ. 2017. Investigating antimalarial drug interactions of emetine dihydrochloride hydrate using CalcuSyn-based interactivity calculations. *PLoS One* 12:e0173303. <https://doi.org/10.1371/journal.pone.0173303>.
46. Schneider-Poetsch T, Ju J, Eyer DE, Dang Y, Bhat S, Merrick WC, Green R, Shen B, Liu JO. 2010. Inhibition of eukaryotic translation elongation by cycloheximide and lactimidomycin. *Nat Chem Biol* 6:209–217. <https://doi.org/10.1038/nchembio.304>.
47. Habibi D, Ogloff N, Jalili RB, Yost A, Weng AP, Ghahary A, Ong CJ. 2012. Borrelidin, a small molecule nitrile-containing macrolide inhibitor of threonyl-tRNA synthetase, is a potent inducer of apoptosis in acute lymphoblastic leukemia. *Invest New Drugs* 30:1361–1370. <https://doi.org/10.1007/s10637-011-9700-y>.
48. Tipparaju SK, Joyasawal S, Pieroni M, Kaiser M, Brun R, Kozikowski AP. 2008. In pursuit of natural product leads: synthesis and biological evaluation of 2-[3-hydroxy-2-[(3-hydroxypyridine-2-carbonyl)amino]phenyl]-benzoxazole-4-carboxylic acid (A-33853) and its analogues: discovery of N-(2-benzoxazol-2-ylphenyl)benzamides as novel antileishmanial chemotypes. *J Med Chem* 51:7344–7347. <https://doi.org/10.1021/jm801241n>.
49. Reader J, van der Watt ME, Taylor D, Le Manach C, Mittal N, Otilie S, Theron A, Moyo P, Erlank E, Nardini L, Venter N, Lauterbach S, Bezuidenhout B, Horatschek A, van Heerden A, Spillman NJ, Cowell AN, Connacher J, Opperman D, Orchard LM, Llinás M, Istvan ES, Goldberg DE, Boyle GA, Calvo D, Mancama D, Coetzer TL, Winzeler EA, Duffy J, Koekemoer LL, Basarab G, Chibale K, Birkholtz LM. 2021. Multistage and transmission-blocking targeted antimalarials discovered from the open-source MMV Pandemic Response Box. *Nat Commun* 12:269. <https://doi.org/10.1038/s41467-020-20629-8>.